Biochimica et Biophysica Acta, 1143 (1993) 319–326

BBABIO 43857

Time-resolved fluorescence spectroscopy and photolysis of the photoreceptor blepharismin

Tomoko Yamazaki [a], Iwao Yamazaki [a], Yoshinobu Nishimura [a], Renke Dai [b] and Pill-Soon Song [b]

[a] *Department of Chemical Process Engineering, Hokkaido University, Sapporo (Japan) and*
[b] *Institute for Cellular and Molecular Photobiology and Department of Chemistry, University of Nebraska, Lincoln, NE (USA)*

(Received 20 November 1992)

Key words Blepharismin, Light signal transduction, Photophobic response, Photoreceptor, Time-resolved fluorescence Photoreaction, (*B japonicum*)

Blepharismin is the photoreceptor for the photophobic response in the ciliate *Blepharisma japonicum* (Scevoli, P, Bisi, F, Colombetti, G, Ghetti, F, Lenci, F, and Passarelli, V (1987) J Photochem Photobiol B Biol 1, 75–84, Lenci, F, Ghetti, F, Gioffre, D, Heelis, P F, Thomas, B, Phillips, G O, and Song, P -S (1989) J Photochem Photobiol B Biol 3, 449–453) Blepharismin was solubilized from the red cells with 2% n-octylglucopyranoside A crude pigment-protein preparation was then successively subjected to Bio-Gel A1 5 filtration, FPLC/hydroxyapatite and FPLC/DEAE ion-exchange chromatography At least two spectrally distinct forms of blepharismin, with the respective absorbance maxima at 597 ± 1 and 601 ± 1 nm, were resolved The steady state fluorescence emission maxima were at 602 5 and 617 5 nm, respectively The fluorescence decay curves for these pigments were non-exponential The major component possesses relatively short fluorescence lifetime (200–500 ps) for the former, according to a global analysis This analysis suggests that the excited state of the shorter wavelength-absorbing form of blepharismin undergoes primary photoprocess faster than that of the free parental chromophore hypericin Photolysis of blepharismin in solution yielded a irreversible product, accompanied by a 10–12 nm bathochromic shift of the absorbance maximum However, the mechanistic nature of the time-resolved fluorescence and the photochemistry of blepharismin remains to be elucidated

Introduction

Along with *Stentor coeruleus*, unicellular ciliate *Blepharisma japonicum* exhibits a photophobic response when stimulated by a sudden increase in light intensity On the basis of the action spectra for the photophobic response [1–3] and for the light-induced electrophysiological responses [4], blepharismin imbedded within the pigment granular organelle has been identified as the photosensor molecule in the photosensory transduction in *Blepharisma japonicum*

Although ethanolic and acetone-extracted pigment preparations of blepharismin have been studied by time-resolved fluorescence measurements [5], the nature of the excited state and the photochemical reactivity of blepharismin in its native protein form remain to be characterized The aim of the present study was to purify the blepharismin protein and to characterize its photoreactivity in terms of picosecond time-resolved fluorescence and visible light photolysis in solution, for a comparative study with the photoreceptor stentorin of the related ciliate *Stentor coeruleus* [6,7]

Correspondence to P -S Song, Department of Chemistry, University of Nebraska, Lincoln, NE 68588, USA

Materials and Methods

Chemicals

Reagents used were obtained from Sigma (St Louis, MO, USA), unless specified otherwise Water for buffer preparations was purified by deionization

Cultures

Cultures of *Blepharisma japonicum* were maintained in open 3-liter beakers containing culture medium at room temperature (22–25°C) The stock cultures were kept in the dark until harvest, and axenic cultures of *Tetrahymena pyriformis* were used as a food source for *Blepharisma japonicum*, as previously described [4]

Isolation and purification of blepharismin

Isolation and purification of blepharismin was based on the modification of the method developed for the

isolation and purification of stentorin from *S coeruleus* [6] Harvested *Blepharisma* was rinsed with culture medium and then centrifuged at 3000 × *g* for 20 min to collect the whole cell pellets Approx 8 ml of extraction buffer containing 20 mM Tris buffer (pH 7 8), 2% n-octylglucopyranoside, 0 5 mM phenylmethanesulfonyl fluoride (PMSF, a serine proteinase inhibitor), 10% sucrose, 10% methyl α-D-mannopyranoside, 1 mM EDTA, and 1 mM dithiothreitol (DTT) was applied for each 1 g pellet The suspension was sonicated for 5 min in a ice bath The resulting solution was further shaken for 10 min and then followed by centrifugation of 27000 × *g* for 30 min to obtain the supernatant as crude extract The pellets were re-extracted with the same amounts of extraction buffer The solution was sonicated for 1 min, shaken for 20 min, and then centrifuged under the same conditions Both supernatants were then combined for chromatographic purification as described below

The FPLC system was comprised of an ISCO model 2350 HPLC pump, model 2360 gradient programmer, UV-5 multiple absorbance detector (ISCO, Lincoln, NE, USA), a Pharmacia 50 ml superloop, and home-packed Amicon Laboratory columns A multiple absorption detection at 280 nm and 580 nm was simultaneously used to record elution profiles for protein and blepharismin, respectively Approx 15 ml of crude extract was loaded on a Bio-gel A1 5 column (2 5 × 45 cm) Elution buffer containing 20 mM Tris (pH 7 8), 0 07% n-octylglucopyranoside, 1 mM EDTA and 1 mM DTT was used to elute blepharismin at a flow rate of approx 0 8 ml/min The 580-nm detectable fraction of pink fluorescence under UV was further applied to a hydroxyapatite column (2 2 × 8 cm) The same elution buffer as before was used to elute the blepharismin at a flow rate of 2 ml/min After the 580-nm-monitored peak was eluted, 0 2 M phosphate buffer (pH 7 8) containing 0 7% n-octylglucopyranoside, 1 mM EDTA, and 1 mM DTT was then applied The 580 nm-monitored fraction was concentrated to 15–25 ml using an Amicon centrifuge tube with 10 kDa cutoff membrane (see Fig 1a)

The resulting solution from the FPLC hydroxyapatite column was further purified through a DEAE cellulose (Sigma) column (2 2 × 8 cm), which was pre-equilibrated with the elution buffer After loading the sample, 20 mM Tris buffer (pH 7 8) was used to collect the void volume fraction, and then a linear gradient from 0 to 1 M NaCl in 20 mM Tris buffer (pH 7 8) was used to elute fraction A1 Following this, 20 mM Mes (2-(*N*-morpholino)ethanesulfonic acid) buffer (pH 6 5) containing 1 M NaCl and 0 3% CTAB was used to elute fraction A2 Without the Mes buffer (pH 6 5), fractions A1 and A2 were not clearly resolved (see Fig 1b, inset) Fraction C was then eluted with 20 mM Mes buffer (pH 5 5) containing 1 M NaCl and 0 5% CTAB Finally, 20 mM acetate buffer (pH 4 5) containing 1 M NaCl, 0 5% CTAB, and 0 7% n-octylglucopyranoside was used to elute fraction D (see Fig 1) SDS-PAGE of various blepharismin preparations were unsuccess-

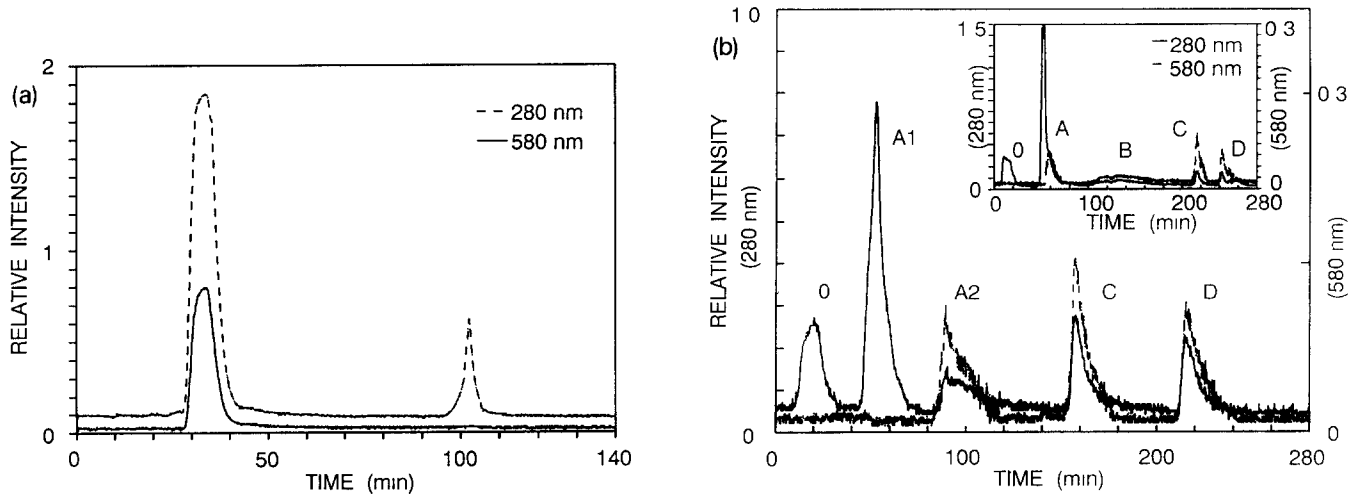

Fig 1 FPLC profiles for blepharismins Absorption of multiple wavelength at 280 nm and 580 nm was simultaneously used to record the profiles (a) FPLC/hydroxyapatite column profile The first fraction was eluted by 20 mM Tris buffer (pH 7 8) containing 0 07% n-octylglucopyranoside The second fraction was eluted with 0 2 M phosphate buffer (pH 7 8) containing 0 7% n-octylglucopyranoside (b) FPLC/DEAE anion-exchange column profile The first fraction was eluted by 20 mM Tris buffer (pH 7 8) with almost non-retention Fraction A1 was eluted with 20 mM Tris buffer (pH 7 8) containing 1 M NaCl After that, a 20 mM Mes buffer (pH 6 5) containing 1 M NaCl and 0 3% CTAB was used to elute fraction A2 Then, fraction C was eluted with 20 mM Mes buffer (pH 5 5) containing 1 M NaCl and 0 5% CTAB Finally, a 20 mM acetate buffer (pH 4 5) containing 1 M NaCl, 0 5% CTAB and 0 7% n-octylglucopyranoside was used to elute fraction D Inset Same as in (b), but without elution with a 20 mM Mes buffer (pH 6 5) Broad band 'B' also contained the chromophore, exhibiting spectral properties similar to those of blepharismin-A2

ful, probably due to (i) low concentrations, (ii) Coomassie blue staining interference by the chromophore, and/or (iii) other unknown anomalies

Photolysis

Samples of blepharismin (primarily blepharismin-A) were prepared by Bio-Gel filtration and hydroxyapatite chromatography Blepharismin solutions in air-tight cuvettes were degassed using standard procedure The irradiation source was a projector light from a 150 W halogen lamp filtered through a 480 nm cutoff filter Absorption spectra of degassed/non-degassed blepharismin solutions were periodically recorded at 4°C on a Shimadzu UV-265 spectrophotometer

Spectral measurements

Absorbance spectra were recorded at room temperature on a Hewlett-Packard 8451A diode array, or a JASCO Ubest 50 spectrophotometer Fluorescence excitation and emission spectra were recorded on a JASCO FP-770 spectrofluorometer The steady-state fluorescence emission spectra of blepharismins, recorded with 530-nm laser excitation, were subjected to global analysis

Time-resolved fluorescence measurements

The picosecond pulsed laser system consists of a mode-locked Nd YAG laser (Spectra Physics 3500), a pulse compressor (Spectra Physics 3690) and a cavity-dumped rhodamine 6G laser (Spectra Physics 3500) The pulse width of the dye laser was about 2 ps (FWHM), and the intensity was 3 4 mW/cm^2 at 4 MHz repetition rate A time-correlated single-photon-counting apparatus [7] was employed to measure fluorescence decays The apparatus was composed of a microchannel-plate photomultiplier (Hamamatsu R2809U-01), a time-to-amplitude converter (Ortec 457), a constant fraction discriminator (Tennelec TC454) and a multichannel pulse-height analyzer (Canberra 35 series) The instrument response function was measured with a pulse width of 30 ps (FWHM) from the scattering light of an aqueous vesicle solution Time-resolved fluorescence emission was recorded in the 12 4-ps step, as described elsewhere [7]

Data analysis global analysis

The time-resolved fluorescence emission spectra were analyzed in terms of multiple emitting components by using the global analysis routine supplied by Professors L Brand and J Beechem [8]

Results

Fig 1a shows the FPLC elution profile of blepharismin extract from a hydroxyapatite column after an initial filtration of the solubilized crude extract through a Bio-Gel A1 5 column A major peak with significant absorbance at 280 and 580 nm was eluted with 0 02 M Tris buffer This fraction was further subjected to

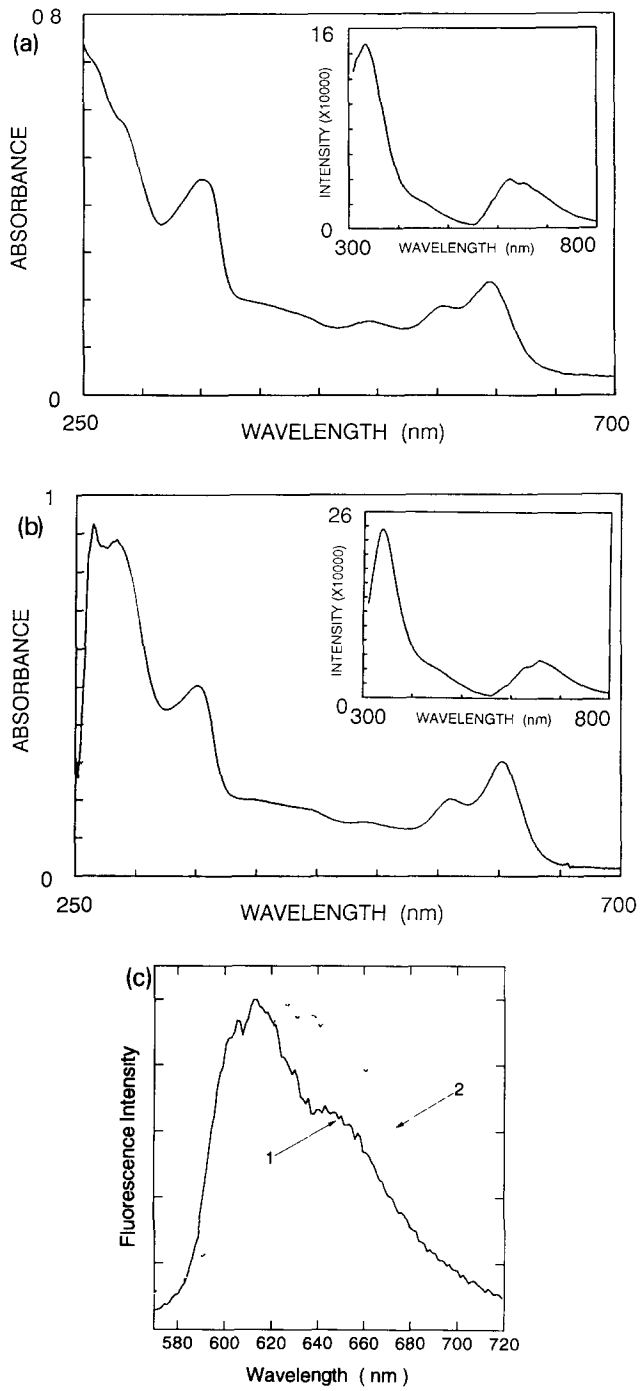

Fig 2 Absorption spectra of blepharismin-A2 (a) and -C (b) in 20 mM Tris buffer (pH 7 8) containing 0 7% n-octylglucopyranoside at room temperature recorded on a HP 8452 diode array spectrophotometer Insets Fluorescence emission spectra of blepharismin-A2 and -C using an excitation wavelength of 280 nm with slit width of 5 nm The sample concentration was kept below about 0 1 at 280 nm in terms of absorbance (c) Fluorescence spectra of blepharismin-A2 (curve 1) and -C (curve 2) Excitation wavelength, 532 nm

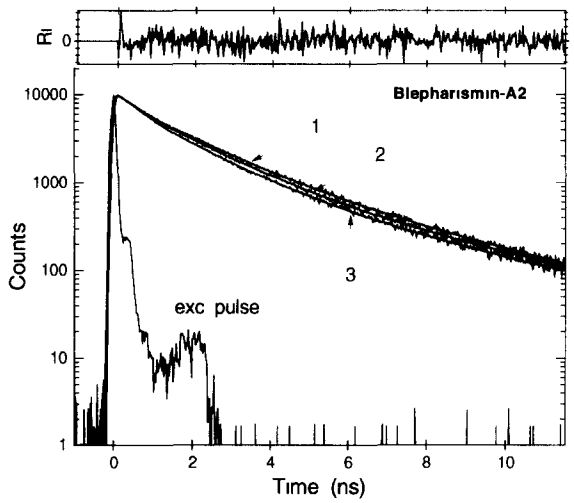

Fig 3 Fluorescence decay curves and calculated best-fit curves (smooth line) for blepharismin-A2 Monitoring wavelengths, 610 nm (curve 1), 650 nm (curve 2) and 690 nm (curve 3) Excitation wavelength, 532 nm The weighted residual curve (R_t) is shown for curve 1 as a typical example

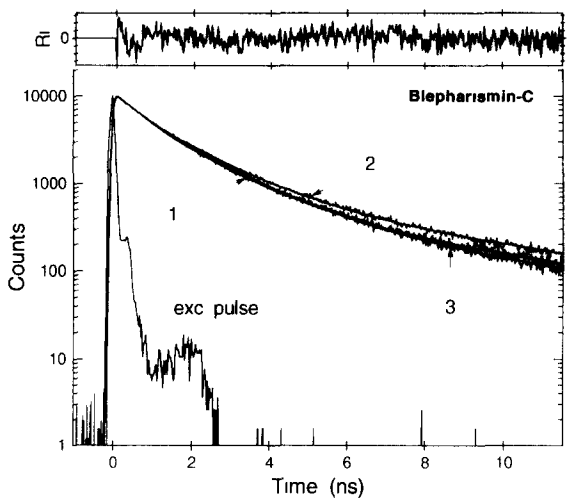

Fig 4 Fluorescence decay curves and calculated best-fit curves (smooth line) for blepharismin-C Monitoring wavelengths, 630 nm (curve 1), 650 nm (curve 2) and 690 nm (curve 3) Excitation wavelength, 532 nm The weighted residual curve (R_t) is shown for curve 1 as a typical example

DEAE ion-exchange chromatography (Fig 1b) In addition to the chromophore-free peak at fraction number 'O' and A1, additional fractions (A2, C, D) with significant absorbance at 580 nm were resolved It is clear that resolution of fraction A2 requires a pH 6 5 buffer, as can be seen in the inset of Fig 1b Spectrally, fractions C and D were essentially identical

Fig 2 shows the absorption spectra of blepharismin-A2 and -C, with absorbance peaks at 280, 554 and 596 (λ_{max}) nm and 284, 350, 560 and 602 (λ_{max}) nm, respectively Their UV fluorescence emission from aromatic amino-acid residues are shown in insets The respective steady-state chromophore fluorescence spectra (Φ_F approx $0\,002 \pm 0\,001$) of blepharismin-A and -C are shown in Fig 2, the latter exhibiting a red shift of the emission maximum relative to the former We found that the shape of the emission spectra is dependent upon excitation wavelength, and vice versa, indicating that more than one emitting component is present in these blepharismin preparations Fig 2c shows the fluorescence emission spectra of blepharismin-A2 and -C recorded with laser excitation at 532 nm

Fig 3 shows the fluorescence decays for blepharismin-A2 at three selected emission wavelengths These decay curves can be best fitted with three emitting components with lifetimes of 4 2–4 7, 1 6–1 7 and 0 4–0 6 ns The intermediate lifetime component represents a major contributor to the fluorescence emission at all wavelengths monitored, whereas the shorter component increases in amplitude with wavelength The longer lifetime component is negligible at 690 nm Blepharismin-C emits fluorescence with similar lifetimes of 6 2–6 3, 1 5–1 6 and 0 4–0 5 ns, but with only a small contribution by the longer lifetime component (Fig 4) Blepharismin-D showed decay parameters sim-

TABLE 1

Fluorescence lifetimes (τ_i), relative amplitudes (A_i) and χ^2 values for blepharismins

	Monitoring wavelength (nm)	τ_1 (ps)	A_1	τ_2 (ps)	A_2	τ_3 (ps)	A_3	χ^2
Blepharismin-A2	590	341	(0 410)	1670	(0 486)	4945	(0 104)	1 215
	610	413	(0 284)	1696	(0 578)	4179	(0 139)	1 125
	650	417	(0 298)	1641	(0 593)	4428	(0 110)	0 998
	690	554	(0 392)	1705	(0 524)	4688	(0 084)	1 080
Blepharismin-C	590	311	(0 433)	1597	(0 504)	5532	(0 064)	1 215
	630	466	(0 352)	1577	(0 597)	6212	(0 051)	1 062
	660	460	(0 341)	1492	(0 586)	6304	(0 073)	1 183
	690	527	(0 423)	1555	(0 523)	6544	(0 054)	1 209

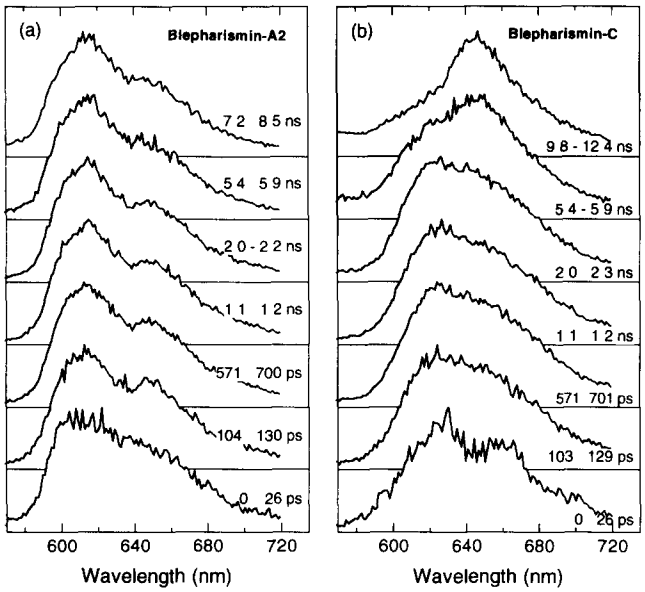

Fig 5 Time-resolved fluorescence spectra of blepharismin-A2 (a) and blepharismin-C (b) Excitation wavelength, 532 nm The time zero corresponds to the time in which the laser pulse reaches the maximum intensity

ilar to blepharismin-A2 and -C, respectively Table I presents fluorescence lifetimes and their amplitudes for blepharismins

To probe the fluorescence decay processes in blepharismin, we recorded time-resolved fluorescence emission spectra (TRS) As described above, the fluorescence decays of the blepharismin preparations exhibited three components The TRS of the fluorescence spectra of blepharismin-A2 showed two distinct changes involving spectral intensity/shape within about 100 ps in blepharismin-A2 and a newly-evolving species emitting at about 650 nm (Fig 5a) The TRS for blepharismin-C shows a significant change in the short time region of 100 ps, and remains roughly constant within about 5 ns, followed by the prominent appearance of a emitting species at about 650 nm (Fig 5b) A major difference between the two TRS for these blepharismin forms is that only blepharismin-C exhibited the long wavelength-emitting band in the time-resolved spectra in the nanosecond range The TRS of the shorter wavelength-absorbing and -emitting species are generally constant over the time range recorded, except between the initial 0–26 and 104–130 ps TRS (Fig 5a), whereas the longer-wavelength-absorbing and -emitting species display significant TRS changes in the later stage of fluorescence emission (Fig 5b)

Global analysis of fluorescence spectra

The TRS differences between the short- and long-wavelength emitters are further confirmed by global analysis of the steady state and by inspection of the TRS spectra Figs 6 and 7 present the results of the

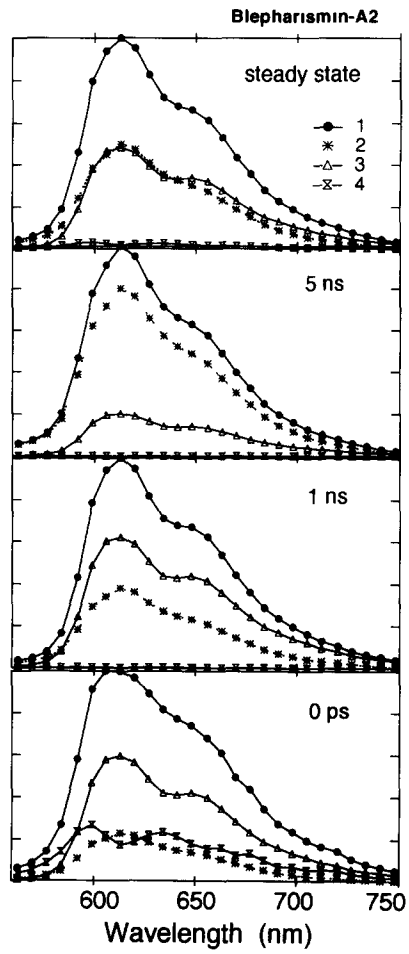

Fig 6 Component analysis for the time-resolved fluorescence spectra and the steady-state spectra obtained by global analysis of the blepharismin-A2 spectrum In each panel, curve 1 is the sum of three components, curve 2 is the 3647-ps component, curve 3 is the 1344-ps component, curve 4 is the 200-ps component

analysis for the two species The steady state and TRS fluorescence spectra of blepharismin-A2 and -C can be resolved in terms of three lifetime components Their lifetime values used in the analysis and the wavelengths of spectral maxima are summarized in Table II It is seen from the figures and the table that, in both cases,

TABLE II

Fluorescence lifetimes and maximum wavelengths of the components derived from the global analysis

	Component	Lifetime (τ) (ps)	Fluor max (nm)
Blepharismin A2	long	3674	613 (650) [a]
	medium	1344	612 (650) [a]
	short	200	598 (634) [a]
Blepharismin C	long	6107	645
	medium	1538	623 (659) [a]
	short	304	634

[a] The wavelength of shoulder in the spectrum

contribution of the short lifetime component to the total spectrum is relatively small In blepharismin-A2, the spectra of medium and long components resemble each other, maxima and shoulders appear at 612 and 650 nm (Table II) A small difference in spectral shape reflects a difference in micro-environments, such as polarity and hydrogen bonding, as seen in hypericin, parent chromophore [9] These two similar spectra give the dominant contribution to the TRS after 100 ps, and results in nearly constant TRS

In blepharismin-C, the spectra of medium and long components (Fig 7) are essentially different, the maximum is located at 623 nm (with a shoulder at 659 nm) for the former, but at 645 nm for the latter In comparison with blepharismin-A2, the spectra shapes of both medium components are similar to each other, but the blepharismin-C spectrum shifts to the red by about 10 nm The 645-nm spectrum, i e , the component, is apparently absent in blepharismin-A2 The TRS of blepharismin-D are similar to those of blepharismin-A2 and -C, respectively (data not shown)

To ascertain the photoreactivity of blepharismin, blepharismin fractionated from the hydroxyapatite chromatography (Fig 1) was photolyzed under anaerobic conditions A slow reaction accompanied spectral changes (red shift from 584 nm to 597 nm, spectral bleaching and an appearance of absorbance at wavelengths longer than 620 nm) (Fig 8a) After prolonged incubation in the dark, the visible absorbance that was lost partially returned (Fig 8b), indicating a slow photoreversibility of the spectral changes observed

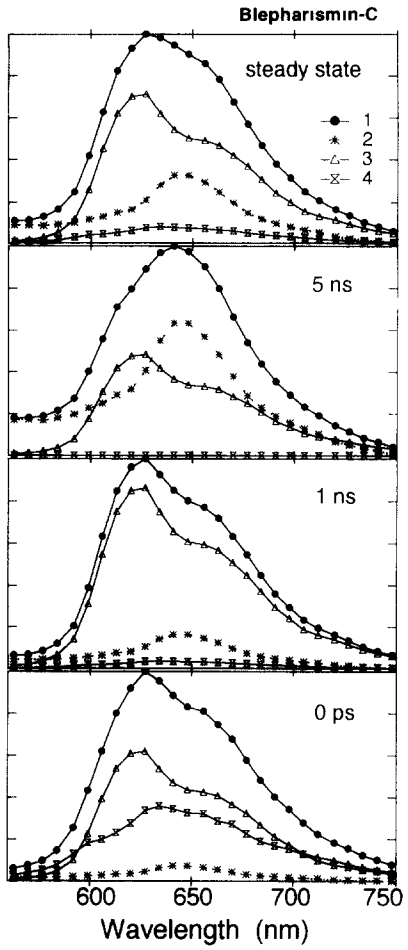

Fig 7 Component analysis of the time-resolved fluorescence spectra and the steady-state spectra for blepharismin-C obtained by global analysis In each panel, curve 1 is the sum of three components curve 2 is the 6107-ps component, curve 3 is the 1538-ps component curve 4 is the 304 ps component

Discussion

The spectroscopic data suggest that blepharismin, isolated and purified using the present experimental protocols, represents heterogeneous pigment protein complexes They exhibit different steady-state and time-resolved fluorescence properties Complexity of blepharismin was further demonstrated by the non-exponential fluorescence decays (Table I) and wavelength-dependent time-resolved fluorescence spectra (Figs 6 and 7) of blepharismin-A2 and other pigment species Crude blepharismin extract showed multi-component fluorescence decays at different pH values [5] What is surprising is that the heterogeneity of the emission process is apparently independent of purifica-

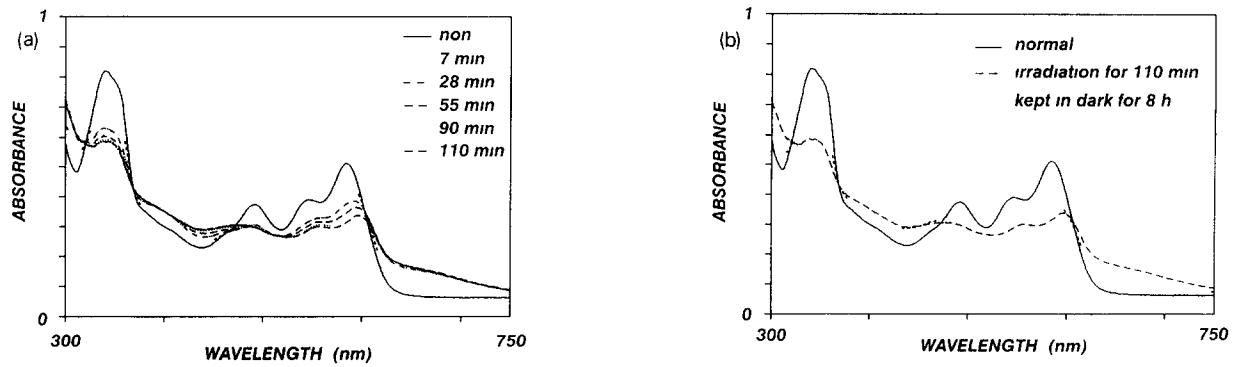

Fig 8 Absorption spectral changes in blepharismin from hydroxyapatite chromatography in Tris buffer (pH 7 8) at 4°C caused by irradiation from a 150 W halogen lamp filtered through a 480 nm cutoff filter (a) Irradiation time as marked (0, 7, 28, 55, 90, 110 min) (b) Partial recovery after 110 min irradiation and then followed by an 8-h dark incubation at 4°C

tion of the pigment preparations Blepharismin-A2 (short-wavelength-absorbing form) exhibits three fluorescence decay components with an increasing contribution of the long-lifetime component at longer wavelengths of emission, whereas blepharismin-C (long-wavelength-absorbing form) shows only a small contribution of the nanosecond longer-wavelength emission In addition, both blepharismin-A2 and -C exhibit relatively slow TRS, 500 ps or later after an exciting picosecond pulse, with the latter showing a marked change in the TRS spectrum at 5–12 ns after the pulse excitation Inspection of the blepharismin-A2 TRS (Fig 5a) shows a gradual red shift of the emission peak during 0–8500 ps time after pulse excitation In blepharismin-C (Fig 5b), the emission maximum shifted to about 650 nm at 9 8–12 4 ns after pulse excitation At first glance these TRS shifts appear to correlate with the TRS spectra of crude blepharismin preparation in ethanolic and aqueous NaOH (20 mM) solutions, respectively [5] It seems possible that the TRS changes in blepharismin-A2 and -C are attributable to a quinonic species [5] or mono-anionic form and a poly-anionic species, which then largely account for the complexity of fluorescence properties of blepharismin as described in this report The ethanolic crude extract (probably protein-free pigment chromophores) from *Blepharisma japonicum* [5] favors the formation of anionic and quinonic isomers of the blepharismin chromophore in the ground state, rather than in the excited state This explains the multi-exponential fluorescence decays in blepharismin However, global analysis shows that at least part of the TRS changes, particularly within 500 ps, is attributable to process(es) occurring in the excited state of blepharismin

With the 645-nm fluorescence band of blepharismin-C, we assign this band to an emission from an anionic species formed in the equilibrium reaction in the ground state The fluorescence excitation spectrum shows a corresponding absorption band of the anionic species around 640 nm The fact that there exists an anionic species in the ground state suggests an important clue on the binding between the chromophore and the protein in blepharismin In the equilibrium of deprotonation reaction of the parent chromophore, hypericin, pK_a value was evaluated to be 11 7 in aqueous solution Since the pH value of the present sample of blepharismin-C is maintained at pH 7 8 in buffer, hypericin should exist predominantly in neutral form It is concluded that there are certain sites on the protein which may lower the pK_a value(s) of the hydroxyl groups

Because the multi-exponential decay and the TRS changes in the blepharismin fluorescence are not straightforward in their interpretations, we performed global analysis on the fluorescence spectra To gain a qualitative insight, we analyzed a limited data set (TRS at 1 18 nm × 6) and reconstructed the TRS (calculated TRS after deconvolution) The calculated TRS spectra showed good agreement with the observed TRS in the time-scale longer than 100 ps The global analysis of the TRS of blepharismin-A2 and -C also revealed that an emitting component appears in the 200–500 ps period after the pulse excitation at all wavelengths of emission was monitored (Fig 6) However, this component does not significantly contribute to the steady state fluorescence spectra of blepharismin Also, the emission spectrum of this component does not match the TRS spectrum of blepharismin-A2 recorded within 100 ps These results of global analysis suggest that a transient species is generated in 200–500 ps after pulse excitation of blepharismin The relatively short fluorescence lifetime component (400–600 ps) of blepharismin may arise from an as yet unidentified reaction(s) occurring from the excited state of the pigment molecule Stentorin I [7] and hypericin [9] exhibit only long-lifetime fluorescence, without significant TRS changes

We now consider the TRS changes at 600–650 nm in 0–500 ps components in blepharismin on the basis of global analysis The analyzed spectra of short components (Figs 6 and 7) exhibit two peaks at 600 and 640 nm with relative intensities being different between blepharismin-A2 and -C We assume here that the short lifetime component consists of two distinct fluorescence bands with a respective maxima at 600 and 640 nm In fact, their lifetimes are different The lifetime monitored at 590 nm includes the fastest decay component of 310–340 ps, but the lifetime monitored at 650 nm is 460–470 ps (Table II) For the 640-nm band there are two possible assignments One is a tautomeric isomer resulting from an intramolecular proton transfer in the excited state It is known that intramolecular proton transfer is so rapid (about 200 fs) that no rise in the fluorescence appears in the ps time resolution An alternative assignment is the same anionic species as the long component of blepharismin-C The fast decay may then reflect this species undergoing a rapid reaction The 600-nm band corresponds well to the fluorescence band of stentorin II [7], i e , functional form of the photoreceptor, which appears in the very short region of the time-resolved fluorescence spectra, representing a fast reaction in the excited state

Blepharismin is likely to be the primary photosensor molecule for the photophobic reaction in *Blepharisma japonicum* [1,2,11] The present study cannot identify which of the blepharismin species resolved by ion-exchange FPLC correspond to biologically functional photoreceptor Unlike stentorin, blepharismin is more photolabile (Fig 8a) which is in agreement with the previous observations Whether or not the slow photochemistry of blepharismin observed is relevant to the light signal transduction process in *Blepharisma japon-*

icum remains to be studied The fact that the observed spectral bleaching induced by irradiation is at least partially reversible suggests that the photochemistry that underscores these spectral changes (Fig 8b) may be important in photosensory transduction or photoadaptation process

Although the nature of the excited state process(es) in blepharismin remains to be elucidated, studies in this laboratory, as well as others [11], have shown blepharismin as a unique photosensor pigment complex that exhibits subnanosecond photochemistry Proton transfer was proposed as a possible primary photoprocess in stentorin, the photoreceptor molecule in the related ciliate *Stentor coeruleus* [7,12–14] However, proton transfer has been ruled out in the excited state of 'free' blepharismin pigment from ethanolic extract of *Blepharisma japonicum*, partly on the basis of a relatively high pK_a^* of the blepharismin chromophore [5], which is considerably higher than the previously reported value of pK_a^* (3 5, [15]) The lower value resulted from the assumption that pH-dependences of the absorbance changes in the UV and near UV region, as well as fluorescence intensity changes at 600–680 nm in hypericin, were due to dissociation of the hydroxyl protons It is now clear that in aqueous solution the spectral changes are complicated by pH-dependent equilibria involving H-bonded and stacked aggregate species of hypericin Nevertheless, proton dissociation remains as a feasible primary process from the excited state of blepharismin, because proton dissociation can be dramatically facilitated by the acid-base network [16,17] of amino-acid residues in the pigment complex or through an intermolecular proton transfer with a suitable proton acceptor [18] To what extent proton transfer takes place during the excited state lifetimes of blepharismin remains to be assessed

Finally, the presence of multiple forms of blepharismin in solution (present work and [11]) is probably photobiologically significant, as the ciliate changes its color from red to blue when exposed to visible light (3–30 W/m^2), with corresponding red shifts in the action spectral maximum for the photophobic response in *Blepharisma japonicum* [19] Recently, a blepharismin-binding protein (BBP) in the range of 35–38 kDa has been partially characterized [11] On the basis of chromatographic behaviors, relative sizes and spectral properties, the blepharismin, A2, corresponds to the holo-BBP protein The shorter-wavelength-absorbing blepharismin A2 and the longer-wavelength-absorbing form of blepharismin, C, may be related to the light-induced color changes in the ciliate

Acknowledgements

This work was primarily supported by a grant from the Army Research Office (No 28748-LS-SM and 29597-LS-EPS) and in part by a U S PHS NIH grant (NS15426) and by the International Scientific Research Program of the Ministry of Education, Science and Culture, Japan (No 03044013)

References

1 Scevoli, P , Bisi, F , Colombetti, G , Ghetti, F , Lenci, F and Passarelli, V (1987) J Photochem Photobiol B Biol 1, 75–84
2 Lenci, F , Ghetti, F , Gioffre, D , Heelis, P F , Thomas, B , Phillips, G O and Song, P -S (1989) J Photochem Photobiol B Biol 3, 449–453
3 Matsuoka, T (1983) J Exp Biol 225, 337–340
4 Fabczak, S , Tao, N , Fabczak, H and Song, P -S (1993) Photochem Photobiol , 57, 889–892
5 Cubeddu, R , Ghetti, F , Lenci, F , Ramponi, R and Taroni, P (1990) Photochem Photobiol 52, 567–573
6 Kim, I -H , Rhee, J S , Huh, J W , Florell, S , Faure, B , Lee, K W , Kahsai, T , Song, P -S , Tamai, N Yamazaki, T and Yamazaki, I (1990) Biochim Biophys Acta 1040, 43–57
7 Song, P -S , Kim, I -H , Florell, S , Tamai, N , Yamazaki, T and Yamazaki, I (1990) Biochim Biophys Acta 1040, 58–65
8 Beechem, J M , Gratton, E , Ameloot, M , Knutson, J R and Brand, L (1991) in Topics in Fluorescence Spectroscopy, Vol 2 (Lakowicz, J R , ed), pp 241–306, Plenum, New York
9 Yamazaki, T , Tamai, N , Nishimura, Y , Yamazaki, I and Song, P -S (1993) J Phys Chem , in press
10 Giese, A (1981) Photochem Photobiol Rev 5, 139–180
11 Gioffre, D , Ghetti, F , Lenci, F and Paradiso, C (1993) Photochem Photobiol , in press
12 Song, P -S (1981) Biochim Biophys Acta 639, 1–21
13 Song, P -S (1983) Annu Rev Biophys Bioengin 12, 35–68
14 Walker, E B , Yoon, M and Song, P -S (1981) Biochim Biophys Acta 634, 289–308
15 Walker, E B , Lee, T Y and Song, P -S (1979) Biochim Biophys Acta 587, 129–144
16 Copeland, R A and Chan, S I (1989) Annu Rev Phys Chem 40, 671–698
17 Kosower, E M (1986) Annu Rev Phys Chem 37, 127–156
18 Falk, H , Meyer, J and Oberreiter, M (1992) Montsch Chem 123, 277–284
19 Checcucci, G , Damato, G , Ghetti, F and Lenci, F (1993) Photochem Photobiol 57, 686–689